

GRAIN BOUNDARY ROTATIONS NEAR CRACK TIPS IN DEFORMED NANOMATERIALS

I.A. Ovid'ko^{1,2,3} and A.G. Sheinerman^{1,2,3}

¹Department of Mathematics and Mechanics, St. Petersburg State University, St. Petersburg 198504, Russia

²Institute of Problems of Mechanical Engineering, Russian Academy of Sciences, Bolshoj 61, Vasilievskii Ostrov, St. Petersburg 199178, Russia

³St. Petersburg State Polytechnical University, St. Petersburg 195251, Russia

Received: June 2, 2014

Abstract. A special mechanism/mode of plastic deformation occurring through stress-driven rotations of low-angle grain boundaries (GBs) near crack tips in nanocrystalline and ultrafine-grained (UFG) materials is theoretically described. It is demonstrated that such rotations of GBs represent energetically favorable processes in wide ranges of parameters characterizing pre-cracked specimens with nanocrystalline and UFG structures. Also, these rotations of GBs in part release high stresses concentrated near crack tips and thus hamper crack growth.

Nanoscale deformation processes occurring in nanowires, micropillars, nanocrystalline and UFG materials represents the subject of intensive research efforts in materials science and physics of nanostructures; see, e.g., [1–17]. In nanocrystalline and UFG bulk solids, specific (inherent to nanostructures) mechanisms/modes of plastic flow effectively operate due to the combined *nanoscale and grain-boundary effects* [2,3,7,8,11,12,14–16]. In nanowires and micropillars having either single crystalline or amorphous structures, the combined *nanoscale and free-surface effects* strongly influence plastic deformation processes and thereby strength and ductility [1,4-7,9,13]. Recently, a particular attention has been devoted to nanowires and micropillars with nanocrystalline and UFG structures as solids where the three effects – the *nanoscale, grain-boundary and free-surface effects* – cooperatively operate, which can cause the actions of unusual modes of plastic deformation [8,10,17,18]. For instance, the experiment [8] revealed GB transformations of a new type – GB rotations – in nanocrystalline Ni nanopillars under a mechanical

load. In Letter [18], GB rotations were theoretically described as stress-driven processes representing a new deformation mechanism in solids. As it has been demonstrated in Letter [18], stress-driven rotations of GBs effectively carry plastic flow and transform GB defect configurations in nanocrystalline nanowires, nanopillars and thin films as well as within subsurface areas of bulk nanocrystalline solids due to the combined actions of the nanoscale, grain-boundary and free-surface effects. Plastic deformation carried by rotations of GBs is accompanied by crystal lattice rotations in the areas swept by rotating GBs [18] and thereby can be treated as a partial case of rotational deformation (defined as plastic deformation accompanied by crystal lattice rotations [19]). Following the experimental data [20–24], crystal lattice rotations intensively occur in vicinities of cracks growing in nanostructured (nanocrystalline or UFG) materials. In the context discussed, it is highly interesting to understand, if stress-driven GB rotations can occur and thereby contribute to the experimentally observed [20–24] crystal lattice rotations in vicinities of cracks grow-

Corresponding author: Ilya Ovid'ko, email: ovidko@nano.ipme.ru

ing in nanostructured materials. The answer to this question is not a trivial extension of the results presented in Letter [18], because there are several peculiarities differentiating the behavior of defects near cracks from that in subsurface areas of nanostructured solids (far from cracks). They are briefly as follows: (i) local stresses are typically much higher near crack tips due to stress concentration, as compared to the subsurface area; (ii) stress distribution is highly inhomogeneous near crack tips due to the effect of the crack, as compared to the subsurface area; (iii) free surfaces associated with a growing crack grow and thus change local stresses in vicinities of cracks, in contrast to conventional (unchanged) free surfaces of solids. The main aim of this paper is to examine and theoretically describe the special mechanism of plastic deformation carried by stress-driven GB rotations near cracks in nanostructured materials. In particular, we will reveal basic characteristics of such rotations and compare them with those of the previously examined [18] GB rotations in subsurface areas of nanostructured materials.

Let us consider the geometric features of plastic deformation mode occurring through stress-driven rotations of low-angle tilt boundaries near cracks in nanostructured solids. Fig. 1a schematically shows a two-dimensional section of a nanostructured solid consisting of nanoscale or ultrafine grains divided by GBs and containing a flat crack. The solid is under a tensile load σ_0 whose direction is normal to the crack plane. The area of the solid near the crack contains a low-angle tilt boundary AB which is presented in the magnified inset in Fig. 1b. The plane of the GB AB makes the angle α with the specimen free surface and has the common point B with the free surface (Fig. 1b). Also, the solid contains static symmetric GBs CA and DA that form the triple junction A with the GB AB (Fig. 1b). We consider the GB AB rotation under the action of the applied load concentrated near the crack tip B, in which case the GB rotates around the triple junction A from the initial position AB to a new position AB' (Fig. 1c). Following the theory of low-angle tilt boundaries [25], the GB AB is represented as a wall of periodically (with a period p) arranged edge perfect dislocations characterized by the same Burgers vector \mathbf{b} (Fig. 1b). We denote the GB rotation angle made by the lines AB and AB' as φ , the length of the GB AB as d , and the crack length as L . We characterize the stress near the crack tip by the stress intensity factor K_I related to the applied load σ_0 and crack length L as $K_I = \sigma_0 \sqrt{\pi L / 2}$. We also assume that

the crack length L is much larger than the distance d , so that in our further calculations the crack can be approximated as a semi-infinite one.

Following [18], the rotation of the GB AB occurs through the cooperative slip of edge dislocations composing this GB in the direction normal to the GB plane AB over various distances in such a way that the rotating GB is flat and thus moves to its new position AB' (Fig. 1c). The GBs AB and AD are unchanged during the rotation of the GB AB. In this situation, their combined role as a stress source is effectively described by a wedge disclination located at the triple junction A and characterized by strength ω [18]. The tilt misorientation angles of the GBs AB, CA, and DA at the triple junction A in the initial state of the system (before the GB rotation; see Fig. 1b) are balanced, in which case the triple junction A does not create stresses. In other words, in the initial state of the defect configuration (Fig. 1b), the long-range stresses created by the edge dislocations composing the GB AB are completely compensated for by the wedge disclination at the triple junction A, that approximates the long-range stresses created by the static GBs CA and AD. In doing so, the disclination strength w is equal by magnitude and opposite in sign to the tilt misorientation θ of the GB AB ($\omega = -\theta$).

During the rotation of the GB, it transforms from symmetric tilt boundary in the initial state (Fig. 1b) into asymmetric one in the final state after the rotation (Fig. 1c). It is related to the fact that the Burgers vectors of GB dislocations change their orientation relative to the GB plane during its rotation. That is, after the rotation of the GB, the Burgers vector of each of its dislocations located at the GB plane AB' has non-zero components parallel and perpendicular to the GB plane AB' (Fig. 1c), in contrast to the initial GB state in which the parallel component is zero (Fig. 1b).

In addition, the tilt misorientation angle of the GB decreases (from θ to θ') due to the GB rotation, because the perpendicular component of Burgers vectors characterizing its dislocations after the GB rotation (Fig. 1c) decreases, as compared to that in the initial GB state (Fig. 1b). The decrease in the tilt misorientation angle violates the balance $\omega = -\theta$ of the misorientation angles of the GBs at the triple junction A, and thereby the junction A becomes a stress source whose elastic energy represents the main hampering force for the GB rotation process.

Also, in the course of the GB rotation, some dislocations approach the surface of the semi-infinite crack and disappear, producing steps at the

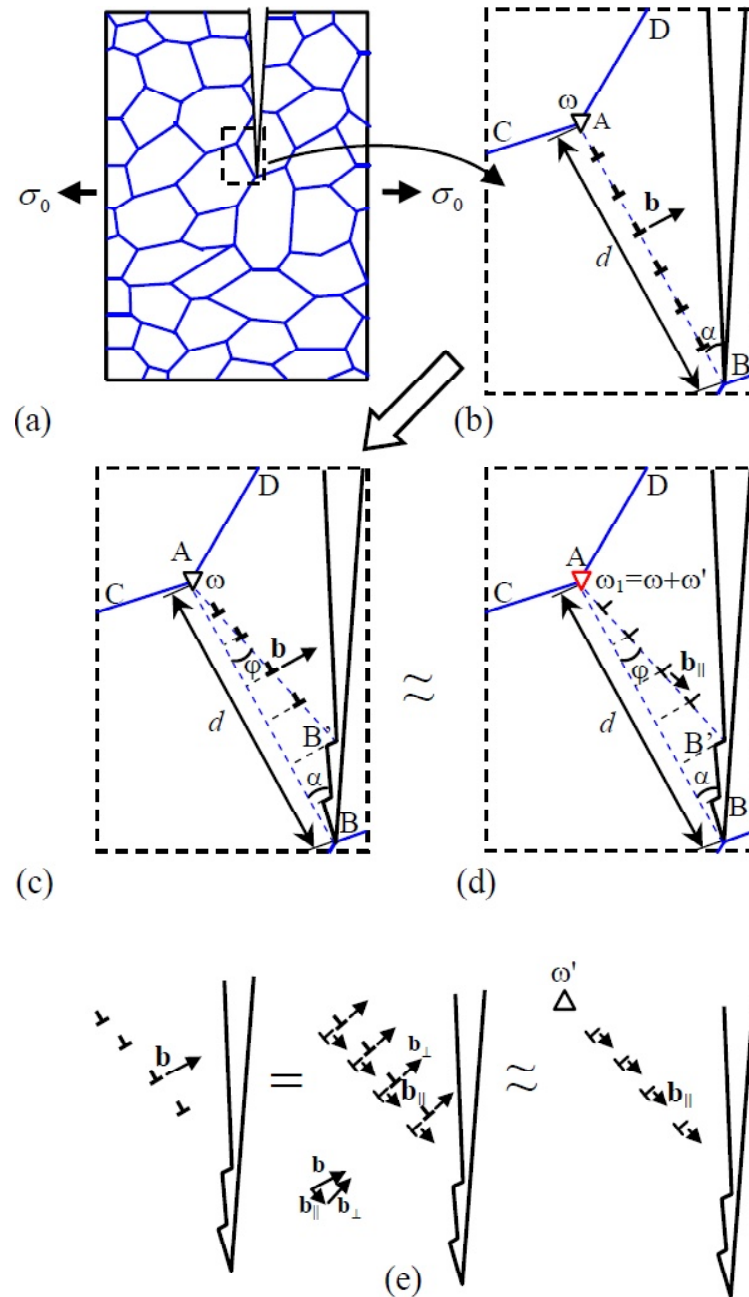


Fig. 1. (Color online) Geometry of grain boundary rotation near a crack in a nanocrystalline specimen. (a) General view of nanocrystalline specimen containing a crack. Figures (b) and (c) show a magnified inset of the region near the crack where stress-driven rotation of a tilt grain boundary occurs. (b) Initial state. A low-angle symmetric tilt boundary AB —a wall of periodically spaced edge dislocations—is located near the free surface and forms a triple junction A with two static symmetric tilt boundaries AC and AD . (c) Stress-driven cooperative motion of GB dislocations occurs which results in tilt boundary rotation (by angle φ) from its initial position AB to a new position AB' . Also, grain boundary rotation leads to the disappearance of several grain boundary dislocations at the crack surface and associated formation of steps at this surface. (d) The defect configuration consisting of both periodically arranged dislocations with the Burgers vectors \mathbf{b} in the rotated dislocation wall and the disclination characterized by the strength ω at the triple junction A is presented as the defect configuration consisting of a pile-up of dislocations with the Burgers vectors \mathbf{b}_{\parallel} , parallel to the plane of the rotated GB and the disclination with the strength $\omega_1 = \omega \sin^2 \varphi$ at the same triple junction (for details, see text). (e) Decomposition of the periodically arranged dislocations with the Burgers vectors \mathbf{b} into a pile-up of dislocations with the Burgers vectors \mathbf{b}_{\perp} , parallel to the plane of the rotated GB, and a wall of dislocations with the Burgers vectors \mathbf{b}_{\parallel} normal to the plane of the rotated GB. The wall of dislocations with the Burgers vectors \mathbf{b}_{\parallel} is approximately equivalent to a wedge disclination with the strength ω' .

crack surface. In general, this affects the critical stress intensity factor for crack advance. However, for simplicity, in the following we neglect the effect of the steps at the crack surface on crack propagation and consider the crack as a flat one. Also, the nanocrystalline specimen is conventionally modeled as an isotropic solid characterized by the shear modulus G and Poisson's ratio ν .

Let us calculate the energy change ΔW (per unit length of dislocations) specifying GB rotation near the crack tip (Figs. 1b and 1c). To do so, for convenience of the calculations, we present each dislocation having the Burgers vector \mathbf{b} as the superposition of the two dislocations characterized by the Burgers vectors \mathbf{b}_\perp and \mathbf{b}_\parallel perpendicular and parallel to the rotating GB plane, respectively (Fig. 1e). The Burgers vectors magnitude b_\perp and b_\parallel are given as: $b_\perp = b \cos \varphi$ and $b_\parallel = b \sin \varphi$, respectively. Also, note that the finite regular wall of the dislocations specified by the Burgers vectors \mathbf{b}_\perp and the period $p/\cos \varphi$ as a stress source is equivalent to a wedge disclination located at the triple junction A and characterized by the strength $\omega' \approx b \cos \varphi / (p/\cos \varphi) = -(b/p) \cos^2 \varphi$ (Fig. 1e). Since $\omega \approx b/p$, we find: $\omega' \approx \omega \cos^2 \varphi$. The superposition of this disclination and the initial disclination located at the triple junction A and characterized by the strength w represents the disclination having the strength $\omega_1 = \omega + \omega' = \omega \sin^2 \varphi$ (Fig. 1d).

As it has been noted previously in this paper, in the initial state of the defect configuration (Fig. 1b), the stresses created by the edge dislocations composing the GB AB are completely compensated for by the wedge disclination located at the triple junction A and characterized by the strength ω . In this case, the initial defect configuration (Fig. 1b) consisting of the dislocation wall AB and the disclination at the triple junction A does not possess any elastic energy. Then the energy change ΔW can be presented as follows:

$$\Delta W = W^\Delta + \sum_{k=1}^N W^d(r_k, \varphi) + \sum_{k=1}^N W_{\text{int}}^{d-\Delta}(r_k, \varphi) + \sum_{k=1}^N \sum_{j=k+1}^N W_{\text{int}}^{d-d}(r_k, r_j, \varphi) - A_e(\varphi) + (N_0 - N) W_{\text{step}}, \quad (1)$$

where N_0 is the initial number of dislocations, N is the number of dislocations after GB rotation, and $r_k = kp/\cos \varphi$ is the distance from the k th dislocation to the triple junction A after GB rotation. Also, in formula (1), W^Δ denotes the proper energy of the disclination A with the strength ω_1 , $W^d(r_k, \varphi)$ is the

proper energy of the k th dislocation with the Burgers vector \mathbf{b}_\parallel , $W_{\text{int}}^{d-\Delta}(r_k, \varphi)$ is the energy of the interaction between the k th dislocation with the Burgers vector \mathbf{b}_\parallel and the disclination of strength ω_1 , $W_{\text{int}}^{d-d}(r_k, r_j, \varphi)$ is the energy of the interaction between the k th and j th dislocations having the Burgers vectors \mathbf{b}_\parallel , $A_e(\varphi)$ is the total work spent by the stress field (created by the applied load in the solid containing the crack (Fig. 1a)) on the motion of all the dislocations with the Burgers vectors \mathbf{b} to either their new positions or the crack surface, and W_{step} is the surface energy of a step created by a dislocation that enters the crack surface (Figs. 1c and 1d).

The expression for the energy W^Δ of the disclination in an isotropic solid with a semi-infinite crack has been calculated previously [26]. The energy W_{step} follows as (e.g., [18]) $W_{\text{step}} = \gamma b$, where γ is the specific surface energy. The other terms in formula (1) have been calculated in the standard way [18] using the known expressions [26,27] for the stresses created by individual dislocations and disclinations in a solid containing a semi-infinite crack (see Appendix A).

As a result, we have calculated the energy change ΔW in the exemplary case of nickel. In our calculations, we have used the following typical values of parameters characterizing Ni [25]: $G = 73$ GPa, $\nu = 0.34$, $b = 0.25$ nm, $\gamma_s = 2.28$ J/m². The dependences of the energy change ΔW on the angle φ of GB rotation are presented in Fig. 2, for the following values of parameters: $\omega = 15^\circ$, $d = 10$ nm, $K_I = 1$ MPa m^{1/2}, and various values of the angle α . The chosen value of K_I is approximately equal to the critical stress intensity factor K_{IC} for brittle fracture. (The latter is given [28] by $K_{IC} = \sqrt{4\gamma G/(1-\nu)}$, which yields: $K_{IC} = 1.004$ MPa m^{1/2}.)

Fig. 2 demonstrates that the curves $\Delta W(\varphi)$ show local oscillations that are, apparently, associated with both the uncertainties in the energies of dislocations located very close (at the distance about one interatomic distance) to the crack surface as well as computational errors. However, with these oscillations neglected, one can see that ΔW first decreases and then increases with increasing φ . For some angle $\varphi = \varphi_{\text{eq}}$ the energy change ΔW is minimum. The equilibrium value φ_{eq} of the angle φ depends on the GB orientation with respect to the GB plane (characterized by the angle α). In particular, when α grows from 30° to 60° , the angle φ_{eq} increases from approximately 4° to approximately 10° . The value $\varphi_{\text{eq}} = 10^\circ$ is large enough and indicates that pronounced GB rotations can occur near crack tips in mechanically loaded solids.

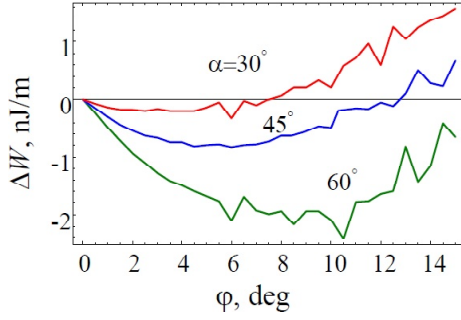


Fig. 2. (Color online) Dependences of the energy change ΔW (characterizing grain boundary rotation near crack) on the rotation angle φ .

We now compare the equilibrium rotation angle φ_{eq} in the case of GB rotation near a crack in nanocrystalline Ni (Fig. 1) and that in the examined previously [18] case of GB rotation near a free surface of nanocrystalline Ni. In the second case, we consider GB rotations near a flat free surface, with the load $\sigma_0 = 0.1D \approx 1.76$ GPa (where $D = G/[2\pi(1 - \nu)]$) being applied in the direction parallel to the free surface. This load creates the shear stress $\tau = 0.05D$ driving the dislocations to move in the planes that make the angle of 45° with the free surface. In this case, for the initial GB length of 10 nm, GB misorientation angle of 11° , the equilibrium GB rotation angle is in the range from 6° to 8° . In the case of GB rotation near a crack, we consider the same values of the applied load, GB misorientation and GB length ($\sigma_0 = 1.76$ GPa, $d = 10$ nm, and $\omega = 11^\circ$, respectively) and various values of the crack length (50 and 207 nm) as well as various values of the angle α between the initial GB plane and crack plane ($\alpha = 45^\circ$ and 60°). The crack lengths of 50 and 207 nm correspond to the stress intensity factors $K_I = 0.493$ MPa m $^{1/2}$ and 1 MPa m $^{1/2}$, respectively.

With our calculations, we found the following results. For $\alpha = 45^\circ$ and $L = 50$ nm, we have: $\varphi_{\text{eq}} = 4^\circ - 6^\circ$. For $\alpha = 45^\circ$ and $L = 207$ nm, we obtain: $\varphi_{\text{eq}} = 6^\circ - 8^\circ$. For $\alpha = 60^\circ$ and $L = 207$ nm, we obtain: $\varphi_{\text{eq}} = 9^\circ - 11^\circ$. For $\varphi_{\text{eq}} = 6^\circ - 8^\circ$ and $L = 1$ μm , which approximately describes a large blunt crack with the length much larger than the Griffith length of a sharp crack, we have: $\varphi_{\text{eq}} = 16^\circ - 18^\circ$. Thus, the equilibrium angle of GB rotation near a crack tip can be much larger than that in the case of GB rotation near a free surface if the crack length is large enough.

To summarize, stress-driven rotations of GBs near cracks represent energetically favorable processes in wide ranges of parameters characterizing pre-cracked nanostructured materials. Depending on the crack length, GB rotations near cracks in pre-cracked materials can be hampered or en-

hanced, as compared to GB rotations near free surfaces of nanostructured materials free from cracks. In particular, when the crack length L is large enough ($L \geq 1$ μm), cracks highly enhance GB rotations.

Note that GB rotations (Fig. 1) in part release high stresses concentrated near crack tips and thus hamper crack growth. Our theoretical estimates of the equilibrium angle φ_{eq} of GB rotations (see above) allow us to conclude that GB rotations (leading to crystal lattice rotations in nanoscale regions) near cracks can significantly contribute to the experimentally observed [20–24] crystal lattice rotations near cracks in nanostructured materials. In parallel with GB rotations, other modes of the rotational deformation can play role in the crystal lattice rotations in question. For instance, the crystal lattice rotations near cracks can be effectively carried by the stress-driven migration of GBs in its conventional “ideal” geometry with the migration direction being perpendicular to the GB plane [29]. At the same time, geometry of the stress-driven GB migration in real nanostructured materials (see, e.g., pioneering experimental works [30,31]) deviates from the “ideal” geometry, and these deviations and associated changes in grain shapes can be described in terms of GB rotations.

ACKNOWLEDGEMENTS

This work was supported, in part, (for IAO) by St. Petersburg State University research grant 6.37.671.2013 and the Russian Foundation of Basic Research (grant 12-01-00291-a), and (for AGS) by the Russian Ministry of Education and Science (Grant 14.B25.31.0017).

APPENDIX A

ENERGY ASSOCIATED WITH GRAIN BOUNDARY ROTATION NEAR A CRACK TIP

In this Appendix, we calculate the terms appearing in expression (1) for energy variation ΔW due to GB rotation near a crack tip (see Fig. 1). The expression for the energy W^Δ (appearing in formula (1)) of the disclination in an isotropic solid with a semi-infinite crack has been calculated previously [26]. It can be presented as $W^\Delta = W^\Delta(d, \alpha, \pi)$, where

$$W^\Delta(r_0, \theta_0) = \frac{\omega_1}{2} \int_0^{r_0} \sigma_{\theta\theta}^\Delta(r, r_0, \theta, \theta_0) \Big|_{\theta=\theta_0} (r_0 - r) dr, \quad (\text{A1})$$

$$\sigma_{\theta\theta}^\Delta(r, r_0, \theta, \theta_0) = 4 \operatorname{Re} \Phi_\Delta \sin^2 \theta + \operatorname{Re} g_\Delta \cos 2\theta + \operatorname{Im} g_\Delta \sin 2\theta, \quad (\text{A2})$$

$$g_{\Delta} = \Phi_{\Delta} + \bar{\Omega}_{\Delta} + (z - \bar{z}) \overline{(\Phi_{\Delta})'}, \quad (\text{A3})$$

$$\Phi_{\Delta}(z) = \frac{D\omega_1}{2} \left\{ \ln(\sqrt{z} - \sqrt{z_0}) - \ln(\sqrt{z} + \sqrt{z_0}) + \frac{\sqrt{z_0} + \sqrt{\bar{z}_0}}{\sqrt{z}} + \frac{z_0 - \bar{z}_0}{2\sqrt{z}(\sqrt{z} + \sqrt{\bar{z}_0})} \right\}, \quad (\text{A4})$$

$$\Omega_{\Delta}(z) = \frac{D\omega_1}{2} \left\{ \ln(\sqrt{z} - \sqrt{z_0}) - \ln(\sqrt{z} + \sqrt{z_0}) + \frac{\sqrt{z_0} + \sqrt{\bar{z}_0}}{\sqrt{z}} + \frac{z_0 - \bar{z}_0}{2\sqrt{z}(\sqrt{z} - \sqrt{\bar{z}_0})} \right\}, \quad (\text{A5})$$

$$z = re^{i\theta}, \quad z_0 = r_0 e^{i\theta_0}, \quad i = \sqrt{-1}, \quad \text{and } D = G/[2\pi(1-\nu)].$$

The energy $W_{\text{int}}^{d-\Delta}(r_k, \varphi)$ is calculated as [32]

$$W_{\text{int}}^{d-\Delta}(r_k, \varphi) = b_{\parallel} \int_{r_k}^l \sigma_{x'y'}^{\Delta}(x', y' = 0) dx', \quad (\text{A6})$$

where $l = d \sin \alpha / \sin(\alpha + \varphi)$ is the length of the GB after its rotation and $\sigma_{x'y'}^{\Delta}$ is the component of the disclination stress in the Cartesian coordinate system (x', y') shown in Fig. A1, which is in the following relation with the disclination stress components in the Cartesian coordinate system (x, y) associated with the crack (see Fig. A1):

$$\sigma_{x'y'}^{\Delta}(x', y') = (1/2)(\sigma_{yy}^{\Delta} - \sigma_{xx}^{\Delta}) \sin[2(\alpha + \varphi)] + \sigma_{xy}^{\Delta} \cos[2(\alpha + \varphi)]. \quad (\text{A7})$$

The components σ_{xx}^{Δ} , σ_{yy}^{Δ} , and σ_{xy}^{Δ} are expressed in terms of the functions Φ_{Δ} and g_{Δ} as [33]

$$\sigma_{xx}^{\Delta} = \text{Re}[4\Phi_{\Delta} - g_{\Delta}], \quad \sigma_{yy}^{\Delta} = \text{Re}[g_{\Delta}], \quad \sigma_{xy}^{\Delta} = -\text{Im}[g_{\Delta}], \quad (\text{A8})$$

where the functions Φ_{Δ} and g_{Δ} are given by (A4) and (A5) with $z = x + iy$ and $z_0 = -de^{i\alpha}$. In turn, the coordinates (x, y) are related to the coordinate x' (at $y' = 0$) appearing in formula (A7) as $x = -h - (l-x') \cos(\alpha + \varphi)$, $y = -(l-x') \sin(\alpha + \varphi)$, where $h = d \sin \varphi / \sin(\alpha + \varphi)$.

The energy $W_{\text{int}}^{d-d}(r_k, r_j, \varphi)$ of the interaction between the k th and j th dislocations with the Burgers vectors b_{\parallel} is calculated as [32]

$$W_{\text{int}}^{d-d}(r_k, r_j, \varphi) = b_{\parallel} \int_{r_j}^l \sigma_{x'y'}^d(x', y' = 0) dx', \quad (\text{A9})$$

where $\sigma_{x'y'}^d(x', y')$ is the component of the stress of the k th dislocation in the Cartesian coordinate system (x', y') shown in Fig. A1, which is in the following relation with the disclination stress components in the Cartesian coordinate system (x, y) associated with the crack (see Fig. A1):

$$\sigma_{x'y'}^d(x', y') = (1/2)(\sigma_{yy}^d - \sigma_{xx}^d) \sin[2(\alpha + \varphi)] + \sigma_{xy}^d \cos[2(\alpha + \varphi)]. \quad (\text{A10})$$

The components σ_{xx}^d , σ_{yy}^d , and σ_{xy}^d are expressed in terms of the complex functions Φ_d and g_d as [33]

$$\sigma_{xx}^d = \text{Re}[4\Phi_d - g_d], \quad \sigma_{yy}^d = \text{Re}[g_d], \quad \sigma_{xy}^d = -\text{Im}[g_d], \quad (\text{A11})$$

where the functions Φ_d and g_d are given [27] by

$$g_d = \Phi_d + \bar{\Omega}_d + (z - \bar{z}) \overline{(\Phi_d)'}, \quad (\text{A12})$$

$$\Phi_d(z) = A \left(\frac{1}{z - z_k} \left(\sqrt{\frac{z}{z_k}} + 1 \right) + \frac{1}{z - \bar{z}_k} \left(\sqrt{\frac{\bar{z}}{z_k}} - 1 \right) \right) + \frac{\bar{A}(z_k - \bar{z}_k)}{2(z - \bar{z}_k)^2} \left(\sqrt{\frac{\bar{z}}{z_k}} + \sqrt{\frac{z}{z_k}} - 2 \right), \quad (\text{A13})$$

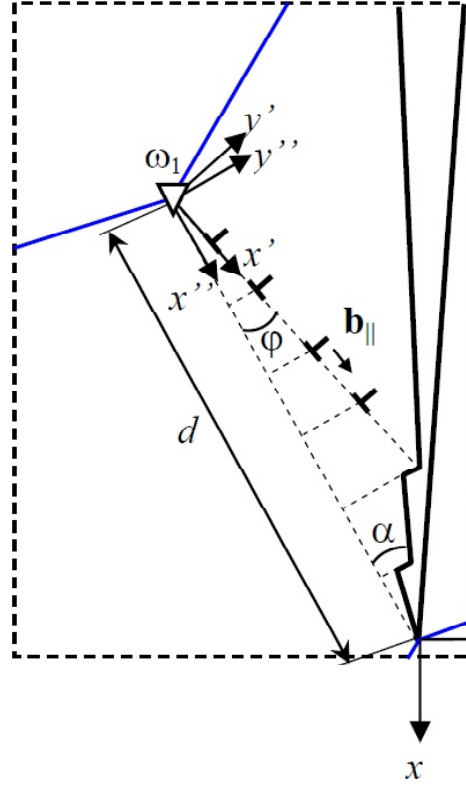


Fig. A1. Geometry of defects in a rotated grain boundary near a crack tip.

$$\overline{\Omega_d(z)} = A \left(\frac{1}{\bar{z} - z_k} \left(\sqrt{\frac{z_k}{\bar{z}}} - 1 \right) + \frac{1}{\bar{z} - \bar{z}_k} \left(\sqrt{\frac{\bar{z}_k}{\bar{z}}} + 1 \right) \right) + \frac{\bar{A}(z_k - \bar{z}_k)}{2(\bar{z} - \bar{z}_k)^2} \left(\sqrt{\frac{z_k}{\bar{z}}} + \sqrt{\frac{\bar{z}_k}{\bar{z}}} + 2 \right), \quad (\text{A14})$$

$z=x+iy$, $z_j=x_j+iy_j$, and $A = Gb_{\parallel} e^{i(\alpha+\varphi)}/[8\pi i(1-\nu)]$. Here the coordinates (x,y) are related to the coordinate x' (at $y'=0$) appearing in formula (A10) as described above.

The proper energy $W^d(r_k, \varphi)$ of the k th dislocation with the Burgers vector \mathbf{b}_{\parallel} can be presented as

$$W^d(r_k, \varphi) = (1/2)W_{\text{int}}^{d-d}(r_k, r_k + b, \varphi) + Db_{\parallel}^2 / 2. \quad (\text{A15})$$

Here the first term on the right hand side of formula (A15) denotes the strain energy of the dislocation while the second term designates the energy of the dislocation core.

The total work $A_e(\varphi)$ of the stress field created by the applied load in the solid with the examined crack (Fig. 1a) done on the motion of all the dislocations with the Burgers vectors \mathbf{b} to their new positions or to the crack surface follows from

$$A_e = -b \sum_{k=1}^{N_0} \int_0^{s_k} \sigma_{x'y'}^e(x'' = r_k, y'') dy'', \quad (\text{A16})$$

where $\sigma_{x'y'}^e(x'', y'')$ is the component of the stress field created by the applied load in the examined solid with a crack in the Cartesian coordinate system (x'', y'') shown in Fig. A1, and s_k is the distance moved by the k th dislocation in the course of GB rotation. The distance s_k follows as

$$s_k = \min\{r_k \tan \varphi, (d - r_k) \tan \alpha\}. \quad (\text{A17})$$

The stress component $\sigma_{x'y'}^e(x'', y'')$ is in the following relation with the stress components in the Cartesian coordinate system (x,y) associated with the crack (see Fig. A1):

$$\sigma_{x''y''}^e(x'', y'') = (1/2)(\sigma_{yy}^e - \sigma_{xx}^e) \sin(2\alpha) + \sigma_{xy}^e \cos(2\alpha). \quad (\text{A18})$$

Using the expressions [28] for the stress field created by a tensile load in an infinite solid with a semi-infinite mode I crack, formula (A18) can be presented as

$$\sigma_{xy}^e(x'', y'') = \frac{K_I}{2\sqrt{2\pi r}} \sin \theta \cos(2\alpha - 3\alpha/2), \quad (\text{A19})$$

where $r = [(d - x'')^2 + (y'')^2]^{1/2}$ and $\theta = \alpha - \pi - \arctan[y''/(d - x'')]$.

The number N of dislocations after GB rotation is calculated as

$$N = \left[\frac{d \sin \alpha \cos \varphi}{\rho \sin(\alpha + \varphi)} \right]. \quad (\text{A20})$$

In formula (A20) ... denotes the integer part, in contrast to other formulae where this sign designates square brackets.

The energy W_{step} follows as (e.g., [18]) $W_{\text{step}} = \gamma b$, where γ is the specific surface energy.

Thus, we have calculated all the terms appearing in formula (1) for the energy variation ΔW associated with GB rotation near a crack tip. This energy is given by formulae (1), (A1)–(A17), (A19) and (A20).

REFERENCES

- [1] M.D. Uchic, D.M. Dimiduk, J.N. Florando and W.D. Nix // *Science* **305** (2004) 986.
- [2] R.Z. Valiev and T.G. Langdon // *Progr. Mater. Sci.* **51** (2006) 881.
- [3] M. Dao, L. Lu, R.J. Asaro, J.T.M. De Hosson and E. Ma // *Acta Mater.* **55** (2007) 4041.
- [4] S.V. Bobylev and I.A. Ovid'ko // *Phys. Rev. Lett.* **103** (2009) 135501.
- [5] Q. Yu, Z.-W. Shan, J. Li, X. Huang, L. Xiao, J. Sun and E. Ma // *Nature* **463** (2010) 335.
- [6] J.H. Luo, F.F. Lu, J.Y. Huang, J.Q. Wang and S.X. Mao // *Phys. Rev. Lett.* **104** (2010) 215503.
- [7] J.R. Greer and J.T.M. De Hosson // *Progr. Mater. Sci.* **56** (2011) 654.
- [8] D. Jang and J.R. Greer // *Scr. Mater.* **64** (2011) 77.
- [9] I.A. Ovid'ko // *Scr. Mater.* **66** (2012) 402.
- [10] N.Q. Chinh, T. Gyori, R.Z. Valiev, P. Szommer, G. Varga, K. Havancsak and T.G. Langdon // *MRS Commun.* **2** (2012) 75.
- [11] X.H. An, S.D. Wu, Z.F. Zhang, R.B. Figueiredo, N. Gao and T.G. Langdon // *Scr. Mater.* **66** (2012) 227.
- [12] K. Edalati, S. Toh, T. Furuta, S. Kuramoto, M. Watanabe and Z. Horita // *Scr. Mater.* **67** (2012) 511.
- [13] O.V. Kuzmin, Y.T. Pei, C.Q. Chen and J.T.M. De Hosson // *Acta Mater.* **60** (2012) 889.
- [14] I.A. Ovid'ko and T.G. Langdon // *Rev. Adv. Mater. Sci.* **30** (2012) 103.
- [15] I.A. Ovid'ko and A.G. Sheinerman // *Rev. Adv. Mater. Sci.* **35** (2013) 48.
- [16] I.A. Ovid'ko and N.V. Skiba // *Rev. Adv. Mater. Sci.* **35** (2013) 96.
- [17] N.Q. Chinh, R.Z. Valiev, X. Sauvage, G. Varga, K. Havancsak, M. Kawasaki and T.G. Langdon // *Adv. Eng. Mater.* (2014), DOI: 10.1002/adem.201300450.
- [18] S.V. Bobylev and I.A. Ovid'ko // *Phys. Rev. Lett.* **109** (2012) 175501.
- [19] M.Yu. Gutkin and I.A. Ovid'ko, *Plastic Deformation of Nanocrystalline Materials* (Springer, Berlin, etc., 2004).
- [20] M. Ke, W.W. Milligan, S.A. Hackney, J.E. Carsley and E.C. Aifantis // *Nanostruct. Mater.* **5** (1995) 689.
- [21] Z. Shan, J.A. Knapp, D.M. Follstaedt, E.A. Stach, J.M.K. Wiezorek and S.X. Mao // *Phys. Rev. Lett.* **100** (2008) 105502.
- [22] S. Cheng, Y. Zhao, Y. Wang, Y. Li, X.-L. Wang, P.K. Liaw and E.J. Lavernia // *Phys. Rev. Lett.* **104** (2010) 255501.
- [23] P. Liu, S.C. Mao, L.H. Wang, X.D. Han and Z. Zhang // *Scr. Mater.* **64** (2011) 343.
- [24] S. Cheng, S.Y. Lee, L. Li, C. Lei, J. Almer, X.-L. Wang, T. Ungar, Y. Wang and P.K. Liaw // *Phys. Rev. Lett.* **110** (2013) 135501.
- [25] J. P. Hirth and J. Lothe, *Theory of Dislocations* (Wiley, New York, 1982).
- [26] N.F. Morozov, I.A. Ovid'ko, A.G. Sheinerman and E.C. Aifantis // *J. Mech. Phys. Solids* **58** (2010) 1088.
- [27] I.-H. Lin and R. Thomson // *Acta Metall.* **34** (1986) 187.
- [28] *Fracture Mechanics and Strength of Materials*, ed. by V.V. Panasyuk Naukova Dumka, Kiev, 1988, vol. 2, In Russian.
- [29] I.A. Ovid'ko, A.G. Sheinerman and E.C. Aifantis // *Acta Mater.* **56** (2008) 2718.
- [30] M. Jin, A.M. Minor, E.A. Stach and J.W. Morris Jr. // *Acta Mater.* **52** (2004) 5381.
- [31] W.A. Soer, J.Th.M. De Hosson, A.M. Minor, J.W. Morris Jr. and E.A. Stach // *Acta Mater.* **52** (2004) 5783.
- [32] T. Mura, *Micromechanics of Defects in Solids* (Martinus Nijho Publishers, Dordrecht, Boston, Lancaster, 1987).
- [33] A.C. Stevenson // *Proc. R. Soc. A* **184** (1945) 129.